ELSEVIER

Journal of Nuclear Materials 248 (1997) 85–90

journal of nuclear materials

Impurity production and transport processes in divertor regions

V.I. Pistunovich *, V.A. Pozharov, D.Yu. Prokhorov

Nuclear Fusion Institute, RRC-Kurchatov Institute, Ulitza Kurchatova 47, 123182 Moscow, Russia

Abstract

2D modelling of the ITER divertor with a lithium target are presented as the first step in the validation of a new divertor concept, based on the capillary structure applied for the cooling of the divertor plates by the evaporation of lithium. The lithium radiative divertor scenario has been examined for the ITER using the DDIC95 code. This code has been specially produced to simulate the behavior of the main plasma and that of impurities, at their arbitrary densities in a real divertor geometry. The self-consistent simulation of a background plasma, neutral gas and impurities is a specific feature of this code. First calculations have shown that the thermal loads on the divertor plates are reduced to 1 MW/m^2. The main power entering the divertor is radiated on the baffles in the divertor. The longitudinal and radial distributions of lithium neutral and ion density are presented in this paper. The lithium flux through the magnetic line near the separatrix and Z_{eff} in the main plasma are estimated. On the basis of the 1D code the fusion plasma parameters inside the separatrix and the values of lithium flow through the separatrix at which the self-sustaining D–T reaction takes place have been calculated. © 1997 Elsevier Science B.V.

1. Introduction

The divertor is the highest loaded element of the tokamak fusion reactor. The main portion of the thermonuclear energy in the ITER is supposed to be irradiated to the walls of the divertor and of the main chamber when argon or the neon are puffed into the divertor. The specific power load of the divertor plates will not exceed 5 MW/m^2 in a steady state operation and 15 MW/m^2 in pulsed mode with 10 s duration of pulses. Nevertheless up to now there is no self-consistent solution of the divertor problem because the heavy gas puffed in the divertor as well as the atoms of the divertor plate structural materials sputtered by the high energy particles will penetrate to the main reactor chamber and they can substantially impair the plasma burning regime. For example, in tokamak experiments the neon puff in the divertor leads to the rise of the hot plasma effective charge. The increase of Z_{eff} in the reactor can extinguish the thermonuclear reactions. So there are no reasons to suppose that the divertor problem will be solved in the ITER by applying the 'sacrificial' materials for the divertor plates such as tungsten, graphite and beryllium.

In the DEMO reactor the situation is more complicated because the thermal loads on the divertor plates become essentially higher and the alternative divertor concept based on the evaporation and radiation seems more probable.

Here calculated results are given in validation of a new divertor concept [1], based on the capillary structure applied for the cooling of the divertor plates by the evaporation of lithium.

2. 2D ITER divertor modelling with lithium targets

A 2D-hydrodynamic code, DDIC95, has been used to simulate a lithium target effect of plasma parameters in the ITER. This code has been specially produced to simulate the behavior of the main plasma and that of impurities, at their arbitrary densities in a real divertor geometry. The self-consistent simulation of a background plasma, neutral gas and impurities is a specific feature of this code.

The background plasma is represented by a set of hydrodynamic equations in the Navier–Stokes form for the flows along the magnetic field and by diffusion equations

* Corresponding author. Fax: +7-095 943 0073; e-mail: vip@wowa.net.kiae.su.

PII S0022-3115(97)00200-6

across the magnetic field. The longitudinal transport is represented by the classical approximation with the flux-limit factor corrections. The transversal transport is simulated, using anomalous transversal coefficients.

The neutral gas is represented by 2D-hydrodynamic Navier–Stokes equations, taking account of neutral–neutral collisions in a model form.

The boundary conditions for the charged component upon a plate are determined from the condition of equality between the hydrodynamic flows and the kinetic ones upon the plate. Calculating the kinetic flows, the present forms of electron/ion distribution functions are used, taking the near-wall potential into account.

The impurities are considered in a multi-fluidal approximation, when each charged state is simulated by a separate fluid.

Different from plates having a carbon or beryllium coating, when the impurity flow from the plate is mainly determined by the processes of target sputtering by incident particles, the lithium flow for the ITER parameters is determined by a thermal flow incident onto the plate. Lithium particles entering the material surface from the plasma are practically not reflected from it. In simulation the material surfaces are assumed to be lithium particles adsorbing on the surface.

Modelling has been done for typical ITER parameters:

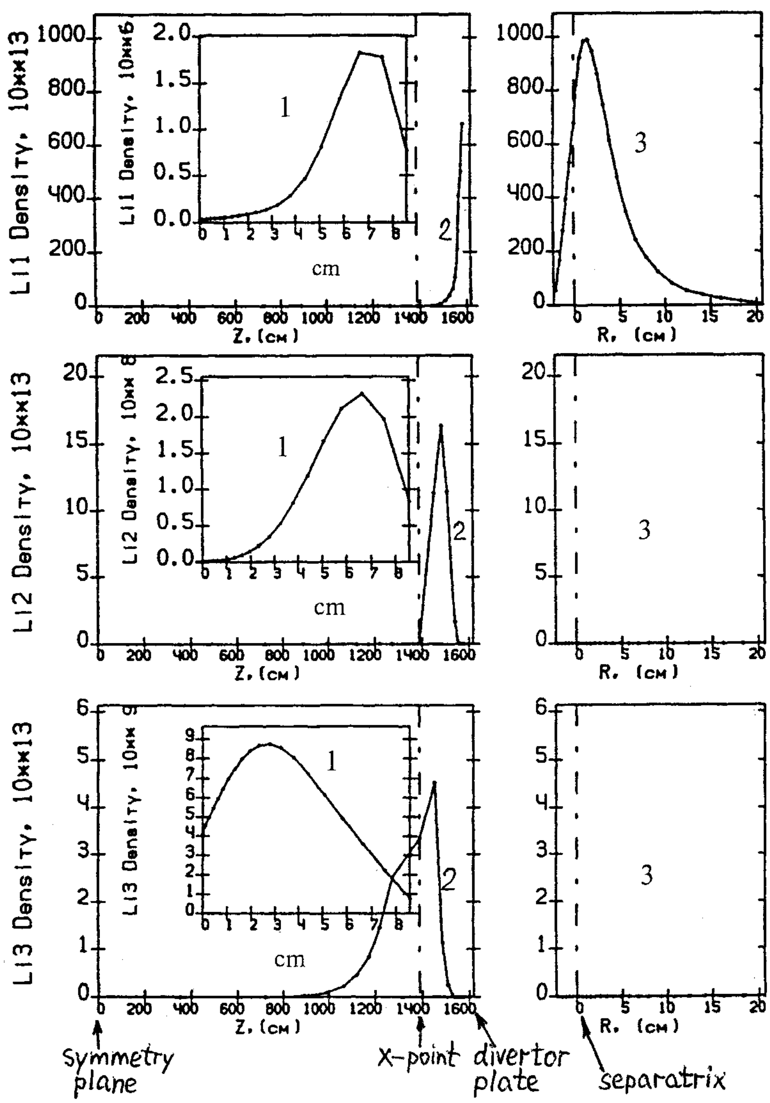

Fig. 1. The spatial distribution of the lithium ion density. (1) Radial distribution in the symmetry plane; (2) distribution along the separatrix and (3) radial distribution on the divertor plate.

energy flow to the divertor layer, -160 MW; electron density at the separatrix, 6×10^{13} cm^{-3} and flux limit factor, 0.21.

The results of the simulation are given as data near an x-point (D^+/T^+ ion density, $n_i^x = 10.7 \times 10^{13}$ cm^{-3}; electron density, $n_e^x = 18.2 \times 10^{13}$ cm^{-3}; ion and electron temperature, $T_i^x = 37.7$ eV, $T_e^x = 105$ eV and $Z_{eff}^x = 1.83$) and on the divertor target: $n_i^d = 0.1 \times 10^{13}$ cm^{-3}, $n_e^d = 6.77 \times 10^{15}$ cm^{-3}, $T_i^d = 1.4$ eV, $T_e^d = 1.4$ eV and $Z_{eff}^d = 1.0$.

The main power which enters the divertor is radiated in the vicinity of the divertor plates by the lithium neutrals which screen the target, reducing the power flow density onto the lithium target to 1.3 MW/m^2. The lithium ion density distributions along the separatrix from the target to the symmetry plane and the radial distribution in the symmetry plane are given in Fig. 1. The lithium ion (Li^+ and Li^{2+}) densities are concentrated in the vicinity of the divertor plate. A noticeable fraction of the Li^{3+} ion density only attains the x-point. In the symmetry plane the Li ion maximal density is about 10^{10} cm^{-3}. The maximal Z_{eff} is attained in the divertor region, Fig. 2, and is considerably reduced in the space between the x-point and the symmetry plane.

The calculations show that the thermal loading onto the divertor plates is essentially reduced without addition of

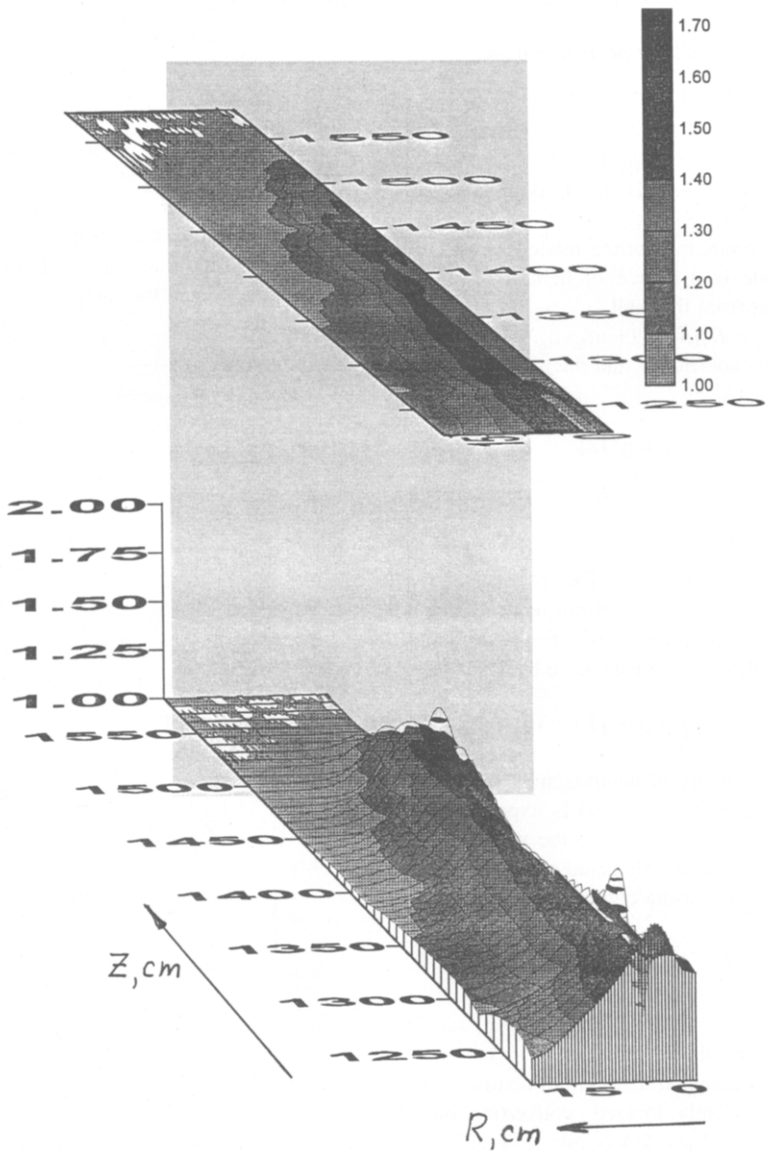

Fig. 2. The spatial distribution of Z_{eff}.

any heavy impurities at the electron density at the separatrix in the symmetry plane $n_e^s = 6 \times 10^{13}$ cm^{-3}. The shielding of the target by lithium evaporation is realized.

3. Effects of lithium and neon fluxes on the ITER-parameters

For determining the fluxes of lithium and neon ions entering the main ITER-plasma from a peripheral zone, 1D-calculations have been done for the ITER-parameters: major plasma radius, $R = 8.14$ m; minor plasma radius, $a = 2.8$ m; plasma current, $I = 21$ MA; elongation, $k = 1.6$; magnetic fields, $B_\nu = 5.68$ T and electron density, $n_e = n_{e0}\, x(1 - x^2)^{0.1}$.

The following equations have been solved.

3.1. Equation of thermalized helium particle balance

$$\partial n_{He}/\partial t = \operatorname{div} \Gamma_{He} + P_{He}, \tag{1}$$

where $P_{He} = f_i^2 n_e^2 \langle \sigma v \rangle /4 + n_e N_{He} I_0$, $f_i = \Sigma z n_e / n_e$, N_{He} is the density of helium neutrals and I_0 is the neutral helium ionization rate.

The first term determines the source related to fusion reaction; the second one is a source of helium neutrals returning after reflection from the wall.

The helium flux $\Gamma_{He} = D_{He} \nabla n_{He} + n_{He} v_{He}$, where D_{He} and v_{He} are the diffusion coefficient and the pinching rate.

$$D_{He} = \chi_e/2, \qquad v_{He} = v^{neo},$$

$$\chi_e = \chi_e^{neo} + \chi_e(T-11 \text{ device scaling}) \ [2],$$

$$\chi_e(T-11 \text{ device scaling}) = 5 \times 10^{19} (T_e/A_i)^{0.5} (n_e q R)^{-1} \times (r/R)^{1.75}\ (\text{cm}^2/\text{s}).$$

The boundary conditions are: $n_{He}(a) = \nabla n_{He}(0) = 0$.

For representing the processes of helium neutral penetration from the wall, the equations for the neutral component distribution in the plasma geometry have been solved:

$$N_{He}(r) = N_{He}(a) \exp(-v_t^{-1}) \int_r^a n_e(\xi) I_0(\xi)\, d\xi,$$

where v_t is the thermal velocity of neutrals and $N_{He}(a)$ is the boundary density of neutrals. $N_{He}(a)$ is expressed in terms of a charged He-flux incident upon the wall, Γ_{He}^{out}.

A flux entering the plasma is calculated as the integral of a helium source over the plasma column periphery:

$$\Gamma_{He}^{in} = a^{-1} \int_0^a n_e(r) N_{He}(r) I_0 r\, dr, \tag{2}$$

$$\Gamma_{He}^{in} = R\, \Gamma_{He}^{out},$$

where R is the helium recycling coefficient.

In a given model it is assumed that helium neutrals are instantaneously and completely ionized, converting into the charged He^{2+}-particles. This allows one to avoid the equation solution for one-fold ionized helium.

3.2. Lithium and neon particle balance equations

These equations are written similar to Eq. (1) but without inner source. The diffusion and pinching rate coefficients are chosen to be the same as those for helium. Since the $T-11$ scaling gives relatively high electron temperatures at the plasma boundary ($T_e \cong 500$–1000 eV), therefore the equations for the charged states, below 7 included, have not been solved for neon ions. The neon source is chosen to be plasma neutrals arriving from the periphery.

The source for lithium has been chosen in three different ways.

(a) Steady along the radius from a to b. One equation is solved in such a case for completely ionized lithium. The source value, S, is found from the following relationship: $S = a\Gamma_{Li}(a)/(a^2 - b^2)$, where $\Gamma_{Li}(a)$ is the varied Li-flux and $\Delta = a - b$ is the divertor layer thickness $\cong$ 13.6 cm.

(b) In this case, a lithium particle gradient is present, $\Delta \cong 4.4$ cm. It is a product from the divertor problem calculations (grad $n_{Li} = 0.01$; 0.1; 0.2×10^{13} cm^{-4} ($R_{He} = 0$); grad $n_{Li} = 0.01 \times 10^{13}$ cm^{-4} ($R_{He} = 0.98$).

(c) As neutrals. The complete set of equations is solved in this case for all the states of ionization. The lithium flux is determined from the relationship similar to Eq. (2).

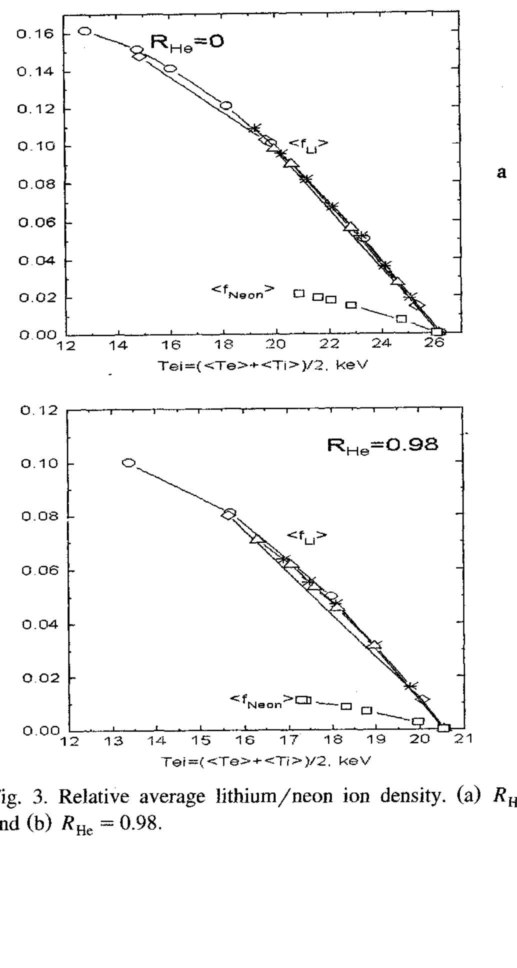

Fig. 3. Relative average lithium/neon ion density. (a) $R_{He} = 0$ and (b) $R_{He} = 0.98$.

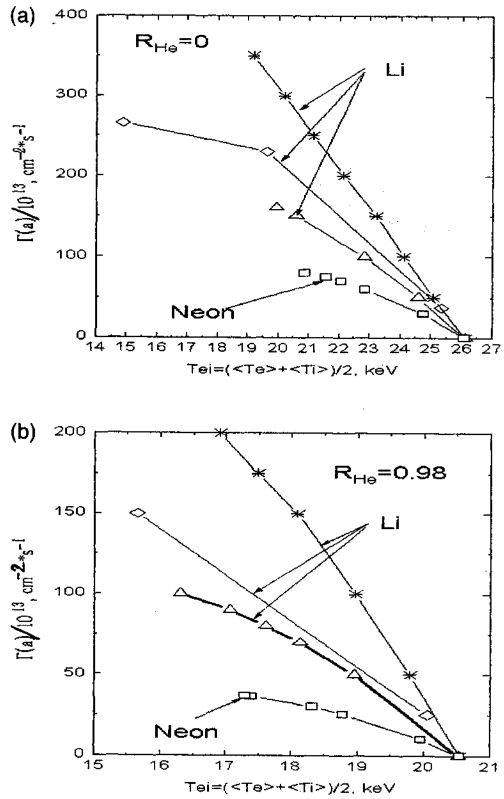

Fig. 4. Li and Ne particle fluxes. (a) $R_{He} = 0$; (b) $R_{He} = 0.98$. (□) Neon; (△) lithium steady source at $\Delta \cong 13.6$ cm; (×) lithium source as neutrals; (◇) lithium steady source at $\Delta \cong 4.4$ cm and (○) lithium steady density.

(d) The Li-particle balance equation is not solved at all, the Li-density is steady across the plasma column.

3.3. The heat conduction equation for electrons and ions

$$\frac{3}{2}\frac{\partial(T_e n_e)}{\partial t} = -\mathrm{div}(q_e + 2.5 T_e \Gamma_e) + Q_{fus}(1-f) - Q_{ei} - Q_{rad} + Q_{oh}, \quad (3)$$

$$\frac{3}{2}\frac{\partial(T_i n_i)}{\partial t} = -\mathrm{div}(q_i + 2.5 T_i \Gamma_i) + Q_{fus} f + Q_{ei}, \quad (4)$$

where $q_e = -\chi_e n_e T_e$ and $q_i = -\chi_i n_i T_i$ are the thermal fluxes of electrons and ions. The f-fraction of the energy transferred by α-particles directly to ions of the main plasma component [3] is expressed as

$$\Gamma_e = -\chi_e / 2\nabla n_e, \qquad \Gamma_i = n_i / n_e \Gamma_e, \qquad \chi_i = \chi_i^{neo}.$$

The boundary conditions are: $T_e(a) = T_i(a) = 100$ eV.

Thus the parameters of the problem are:

1. Electron density.
2. Helium recycling coefficient.
3. Lithium source flux.

All the calculations have been done with the fixed Troyon coefficient g_{tr}, $g_{tr} = \beta_{tor}(\%) a(\mathrm{m}) B(\mathrm{T}) / I_p(\mathrm{MA}) = 2.5$, where the contribution of fast α-particles is not taken into account.

The amount of lithium-accumulated in the plasma under the same fluxes, $\Gamma(a)$, is determined by the distance to which the source is shifted into the plasma. The greater the source width, the better the lithium confinement and, as a result, the limiting permissible flux will be smaller (Figs. 3 and 4). In the case (a) ($\Delta \cong 13.6$ cm) the poisoning with lithium starts at the volume-averaged concentration of lithium $\langle f_{Li} \rangle = \langle N_{Li} \rangle / \langle N_e \rangle = 7\%$ ($R = 0.98$) and $\langle f_{Li} \rangle = 9.8\%$ ($R = 0$) that correspond to the fluxes 1×10^{15} and 1.6×10^{15} cm^{-2} s^{-1}, respectively. The $T-11$ scaling assumes an inverse dependence of χ_e on the electron density, and therefore, with a rise in n_e, the Li and Ne-particle diffusion coefficients are reduced which results in quenching of the fusion reaction burn during the attempts to produce high fluxes. In case of presenting the source as the entry of Li-neutrals, the flux limit starts to take place somewhat later (2×10^{15} cm^{-2} s^{-1} ($R_{He} = 0.98$) and 3.5×10^{15} cm^{-2} s^{-1} ($R_{He} = 0$)). Presenting the gradient (case (c)), the fluxes occupy intermediate values.

The main plasma characteristics at the fluxes close to the critical ones are given in Table 1.

Table 1
The main plasma characteristics at the fluxes close to the critical ones

Type of source	Neon				Lithium			
	neutrals		steady, $\Delta \cong 13.6$ cm		neutrals		steady, $\Delta \cong 4.4$ cm	
$\Gamma(a)$ (10^{15} cm^{-2} s^{-1})	0.8	0.365	1.6	1.0	3.5	2.0	2.66	1.5
R_{He}	0.0	0.98	0.0	0.98	0.0	0.98	0.0	0.98
$\langle n_e \rangle$ (10^{13} cm^{-3})	6.9	8.4	7.25	9.0	7.67	8.56	10.1	9.4
$\langle T_e \rangle$ (keV)	19.1	16.54	18.5	15.7	20.5	16.24	14.3	15.5
$\langle T_i \rangle$ (keV)	22.7	18.06	21.4	16.9	26.5	7.6	15.4	16.2
Z_{eff}	2.97	2.4	1.64	1.67	1.74	1.63	1.94	1.72
τ_E (s)	10.6	14.6	10.1	13.8	11.0	3	16.8	14.8
Q_{fus} (MW)	315	266	270	232	265	237	228	227
Q_{rad} (MW)	196	176	143	140	147	139	153	140
$\langle f_{He} \rangle$ (%)	3.34	14.6	3.0	12.4	3.0	12.6	3	12
$\langle f_{Ne} \rangle$ (%)	2.10	1.1	40.0	0.0	0.0	0.0	0.0	0.0
$\langle f_{Li} \rangle$ (%)	0.0	0.0	19.8	7.1	11	6.37	14.8	8.0
τ_{He} / τ_E	0.8	3.7	0.88	3.03	0.88	3.98	0.9	3.82
Q_{rad} / Q_{fus}	0.62	0.67	0.6	0.6	0.56	0.59	0.67	0.63

4. Conclusion

The calculations to base the new ITER divertor concept with liquid lithium have been done. This concept assumes the evaporation–radiation cooling of the divertor as the most loaded part of the reactor.

2D modeling of the ITER divertor with a lithium target is made as a first step in the validation of a new divertor concept. The lithium radiative divertor scenario has been examined for the ITER using the DDIC95 code. The calculations have shown that thermal loads on the divertor plates are reduced down to 1.3 MW/m^2. The main power entering the divertor is radiated on the baffles in the divertor. The longitudinal and radial distributions of lithium neutral and ion density are calculated.

On the basis of radial Li-ion density distributions in the divertor layer one-fold calculations of the ITER-plasma parameters inside the separatrix have been done.

The limiting Li-ion fluxes arriving from the peripheral zone to the main reactor plasma, starting from where the DT-reaction quench in ITER occurs, have been determined. The calculations take account of helium recycling in the reactor.

Similar calculations have been done with neon, for comparison.

From the calculations it follows that the critical density of lithium in the peripheral reactor zone can be about seven times greater than the Ne-density at which the DT-reaction quench occurs.

These results promise the creation of a pure main plasma in the reactor tokamak with the lithium divertor.

References

[1] L.G. Golubchikov, V.A. Evtikhin et al., J. Nucl. Mater. 233–237 (1996) 667.

[2] V.G. Merejkin, V.S. Mukhovatov, A.R. Polevoi, Sov. J. Plasma Phys. 14 (2) (1988) 69.

[3] V.I. Pistunovich, At. Energ. 35 (7) (1973).